

BOPIM: Bayesian Optimization for influence maximization on temporal networks

Eric Yanchenko

Abstract—The goal of influence maximization (IM) is to select a small set of seed nodes which maximize the spread of influence on a network. In this work, we propose BOPIM, a Bayesian Optimization (BO) algorithm for IM on temporal networks. The IM task is well-suited for a BO solution due to its expensive and complicated objective function. We propose a simple surrogate function to model the objective function and leverage Gaussian Process regression with shrinkage priors to fit the model. An acquisition function based on the median of the posterior distribution leads to a straightforward procedure to select the next sampling point. In numerical experiments on real-world networks, we find that, on average, the surrogate function estimates the true influence spread within a few nodes. Additionally, we show that BOPIM yields comparable influence spreads to a gold-standard greedy algorithm while being as much as seventeen times faster. We also use these experiments to demonstrate the proposed method's ability to quantify uncertainty in optimal seed sets. To the knowledge of the author, this is the first attempt to look at uncertainty in the seed sets for IM, as well as the first application of BO to a constrained, combinatorial optimization problem.

Index Terms—Diffusion, Dynamic networks, Shrinkage priors, Uncertainty quantification



1 INTRODUCTION

Influence maximization (IM) is a canonical network science problem where the goal is to select a small set of seed nodes in order to maximize the influence spread on a graph [1], [2]. Over the past two decades, IM has garnered significant research interest due to its relevance in online marketing campaigns [3], [4], [5], rumor spreading [1], [6], public health campaigns [7], [8], [9], [10], vaccine strategies [11], [12], and more. Traditionally, the problem assumes the graph to be static, i.e., nodes and edges are fixed. In many situations, however, this may be unrealistic. For example, consider a marketing campaign on Twitter where a company promotes a new product. As users and followers change daily, an effective IM algorithm must account for this dynamism. Therefore, recent work has looked at the IM problem on temporal networks [13] where edges change with time. Some methods use a greedy algorithm and probabilistic approximation of the expected influence spread [14], [15], [16], while others eschew costly influence spread calculations by simply ranking nodes in order of importance [6], [17], [18]. We refer the interested reader to [19] for a review of temporal IM.

Separate from the IM problem, Bayesian Optimization (BO) has emerged as a popular paradigm for optimizing complicated objective functions [20], [21], [22]. Machine learning hyper-parameter tuning [20], [23], [24] and experimental design [21], [25], [26] are just a few of the many applications where BO has been successfully implemented. BO approximates a complicated objective function with a simple surrogate function and fits this model via Bayesian regression. The statistical model is maximized with an ac-

quisition function before evaluating this new point on the original objective function. Finally, this point is added to the data set and the process repeats.

In this work, we propose BOPIM, a novel BO algorithm for IM on temporal networks. We construct an intuitive surrogate model for the influence spread function, compare three popular shrinkage priors to fit this model, and implement a simple acquisition function to select the next candidate point. In numerical experiments on real-world networks, BOPIM yields seed sets with influence spreads comparable to those of a greedy algorithm but at a fraction of the computational time. Additionally, the BO algorithm yields measures of uncertainty on the seed sets. To the knowledge of the author, this is the first application of BO to a constrained, combinatorial optimization problem as well as first attempt to quantify the uncertainty in seed sets. Indeed, the proposed algorithm is also one of the few approaches to tackle the IM problem from a statistical angle.

The layout of the paper is as follows. For the remainder of Section 1, we introduce notation and give a formal problem statement. Section 2 presents the main algorithm while Section 3 is devoted to numerical experiments. We share concluding thoughts and future directions in Section 4.

1.1 Notation and problem statement

Let $\mathcal{G} = (G_1, \dots, G_T)$ be a temporal graph where a graph snapshot $G_t = (V, E_t)$ is defined by node set V and edge set E_t . We let $|V| = n$ be the number of nodes and define $m = |\cup_{t=1}^T E_t|$ as the number of unique edges. Given an influence diffusion process and integer $k < n$, the goal of IM is to find a set of nodes S with $|S| = k$ such that if the nodes in S are “influenced” at time $t = 1$, then the spread of influence at time $T + 1$ is maximized.

Central to this problem is the influence diffusion mechanism. Some of the most popular choices are the Indepen-

• E. Yanchenko: Department of Statistics at North Carolina State University, USA, and Department of Computer Science at Tokyo Institute of Technology, Japan. E-mail: ekyanche@ncsu.edu

dent Cascade (IC) [27], [28] and Linear Threshold [29], [30] models. We adopt the Susceptible-Infected (SI) model from epidemiological studies [6], [15]. In the SI model, a node is either in a susceptible (S)¹ or infected (I) state. A node is infected if it was influenced at some point during the process, and susceptible otherwise. At time $t = 1$, nodes in the seed set are set to state I, and all other nodes initialize to state S. At time t , a node in state I attempts to influence all of its neighbors. Specifically, if node i is in state I, node j is in state S, and there exists an edge between node i and j at time t , then node j will be in state I at time $t + 1$ with probability λ . The process concludes at time $T + 1$ and the number of nodes in state I corresponds to the total influence spread. If we let $\sigma(S)$ be the expected number of influenced nodes at time $T + 1$ for seed set S , the IM problem seeks the set of nodes of size k that maximizes $\sigma(S)$ on \mathcal{G} , i.e.,

$$S^* = \arg \max_{S \subseteq V, |S|=k} \sigma(S). \quad (1)$$

The IM problem has been shown to be NP-hard under many popular diffusion mechanisms [31] so finding the global optimum by brute-force calculation is infeasible even for moderate n . Indeed, as the influence spread function is typically computed using Monte Carlo (MC) simulations, even evaluating $\sigma(S)$ is costly. Many IM algorithms efficiently compute the influence spread function and apply a greedy algorithm to choose the seed nodes, while others skip evaluation of the objective function and instead use a heuristic to rank nodes by influence. In the remainder of this work, we describe a BO algorithm to approximate the solution in (1).

2 BAYESIAN OPTIMIZATION

We now present the main contribution of this paper, the BOPI algorithm, by addressing the three main steps of the BO schema: the objective function, statistical model and acquisition function.

2.1 Objective function

The first step in a BO algorithm is the initial evaluation of the objective function. Let $f : \mathcal{X} \rightarrow \mathbb{R}$ be some real-valued function defined on domain \mathcal{X} that we wish to maximize. BO is particularly useful when $f(\cdot)$ is computationally expensive to evaluate, lacks special structure, e.g., concavity, and/or has unavailable first and second order derivatives. Then we evaluate $f(\mathbf{x}_i)$ for $\mathbf{x}_i \in \mathcal{X}$ and $i = 1, \dots, N_0$ for a user-defined N_0 .

For the temporal IM problem, let $\mathbf{x} \in \mathcal{X} = \{0, 1\}^n$ be such that $x_j = 1$ if node j is in the seed set, and 0 otherwise, for $j = 1, \dots, n$. Since the seed set is limited to k nodes, we impose the constraint that $\sum_{j=1}^n x_j = k$. Then we define $f(\mathbf{x})^2$ as the expected influence spread for seed set \mathbf{x} . We stress that $f(\cdot)$ is highly dependent on \mathcal{G} as well as the diffusion process, but suppress this in the notation for convenience. $f(\cdot)$ is an ideal candidate for BO because its evaluation does not yield derivatives and it is

expensive to compute via MC simulations. For the initial N_0 evaluations of $f(\cdot)$, we remark that nodes with high degrees on the temporally aggregated network, $\tilde{G} = \cup_t G_t$, are good candidates for the optimal seed set. Therefore, instead of randomly sampling \mathbf{x}_i from \mathcal{X} , we sample nodes *proportionally to their degree*. Mathematically, this means sampling k times without replacement from a distribution with probability mass function $P(Z = j) = d_j / \sum_k d_k$ where d_j is the degree of node j on \tilde{G} for $Z \in \{1, \dots, n\}$. This sampling scheme ensures that the model better fits the objective function near the expected optimal seed set (see Section 3.2 for empirical evidence). With $\mathbf{x}_1, \dots, \mathbf{x}_{N_0}$ sampled, we define $\mathbf{X} = (\mathbf{x}_1^T, \dots, \mathbf{x}_{N_0}^T)^T \in \{0, 1\}^{N_0 \times n}$ and evaluate $f(\mathbf{x}_i)$ using MC simulations.

2.2 Statistical model

Next we need an adequate surrogate model for the objective function. The most popular approach uses *Gaussian Process (GP)* regression. Let y_i be the observed evaluation of the objective function. Assuming we observe values with some uncertainty, we have

$$y_i = f(\mathbf{x}_i) + \varepsilon_i, \quad (2)$$

where $\varepsilon_i \stackrel{\text{iid}}{\sim} \text{Normal}(0, \sigma^2)$ for $i \in \{1, \dots, N_0\}$. Now, we construct a surrogate model $f_\beta(\mathbf{x})$ of $f(\mathbf{x})$ parameterized by β . Motivated by [32], we assume that the surrogate model is linear in its parameters, i.e.,

$$f_\beta(\mathbf{x}_i) = \sum_{j=1}^n x_{ij} \beta_j = \mathbf{x}_i \beta \quad (3)$$

for $\beta = (\beta_1, \dots, \beta_n)^T$. GP regression uses a multivariate normal prior $\beta \sim \text{Normal}(\mathbf{0}_n, \Sigma)$ where $\mathbf{0}_n$ is the vector of zeros of length n and Σ is some covariance matrix. We also empirically standardize $\mathbf{y} = (y_1, \dots, y_{N_0})^T$ to have mean zero to remove the need for an intercept.

Since n is large for most real-world networks, the dimension of β will also be large. Additionally, it is unlikely that each component of β is significant, i.e., many nodes inclusion in the seed set does not lead to significant influence spread. Thus, we endow β with a *sparsity-inducing shrinkage prior*. We consider three such priors: Horseshoe, Dirichlet-Laplace and R2D2. Each of these frameworks is designed to shrink insignificant coefficient estimates towards zero while still allowing for accurate estimation of the important coefficients. All methods have efficient Gibbs samplers reported in the Supplemental Materials.

2.2.1 Horseshoe prior

The Horseshoe (HS) prior [33], [34] handles sparsity via a half-Cauchy prior distribution on the variance of the coefficients. Specifically,

$$\begin{aligned} \beta_j | \lambda_j^2, \tau^2, \sigma^2 &\sim \text{Normal}(0, \lambda_j^2 \tau^2 \sigma^2) \\ \lambda_j^2, \tau^2 &\sim C^+(0, 1) \end{aligned} \quad (4)$$

where $j = 1, \dots, n$ and $C^+(0, 1)$ is the standard half-Cauchy distribution. Thus, τ^2 represents the global shrinkage and λ_j^2 controls the local shrinkage of each coefficient. For the Gibbs sampler, we leverage an auxiliary variable formulation [35].

1. We use S to refer both to the susceptible state and seed set, but from context the usage should be clear.

2. $f(\mathbf{x}) = \sigma(S)$ if $x_j = 1$ whenever $j \in S$, and 0 otherwise.

2.2.2 Dirichlet-Laplace prior

Another popular shrinkage prior is the Dirichlet-Laplace (DL) prior [36]. This model is:

$$\begin{aligned} \beta_j | \phi_j, \tau &\sim \text{DE}(\phi_j \tau) \\ \phi &= (\phi_1, \dots, \phi_n) \sim \text{Dirichlet}(a, \dots, a) \\ \tau &\sim \text{Gamma}(na, 1/2) \end{aligned} \quad (5)$$

where $j = 1, \dots, n$ and $\text{DE}(\cdot)$ is the double exponential (Laplace) distribution. The parameter ϕ determines the local importance of each coefficient while τ controls the overall variance in the linear predictor.

2.2.3 R2D2 prior

Recently, the R2D2 prior [37], [38] has proven to be an excellent method for variable selection, both theoretically and empirically. The R2D2 prior is formulated as:

$$\begin{aligned} \beta_j | \phi_j, \omega &\sim \text{DE}\{\sigma(\phi_j \omega / 2)^{1/2}\} \\ \phi &= (\phi_1, \dots, \phi_n) \sim \text{Dirichlet}(a_\pi, \dots, a_\pi) \\ \omega &\sim \text{BP}(a, b) \end{aligned} \quad (6)$$

where $j = 1, \dots, n$ and $\text{BP}(a, b)$ is the beta-prime distribution. Similar to DL, the ϕ controls the local shrinkage of each component while ω controls the global shrinkage.

2.2.4 Coefficient interpretation

The coefficient β_j represents the marginal importance of each node to the overall influence spread. This means that if the estimate of β_j is positive and large, then including node j in the seed set leads to a larger total influence spread. Conversely, small and negative coefficient estimates correspond to nodes whose inclusion in the seed set does not yield large influence spreads. We stress, however, that the coefficient estimates are *not* interpretable in the traditional sense. Typically, the coefficient β_j for a binary explanatory variable $x_j \in \{0, 1\}$ corresponds to the increase in the response when $x_j = 1$ and all other variables are fixed. This interpretation is invalid in our context, however, due to the constraint $\sum_{j=1}^n x_j = k$. In other words, β_j does not correspond to the increase in the influence spread if node j is added to the seed set and all other nodes are held fixed, because then the number of nodes in the seed set would be greater than k . While the estimates are not interpretable, they do yield a relative sense of the increase/decrease of the objective function if a node is seeded, and in this sense, are analogous to a node-ranking heuristic.

2.3 Acquisition function

With regression model in hand, we turn our attention to the acquisition function. Each coefficient β_j represents the marginal importance of including node j in the seed set. So if β_j is much greater than zero, then seeding node j leads to a relatively large value of the objective function. Therefore, selecting the k nodes with largest β_j estimate maximizes the surrogate function $f_\beta(\mathbf{x})$ under the constraint that $\sum_{j=1}^n x_j = k$. In practice, the posterior distribution of β_j often has a large variance so we suggest the posterior median as a robust measure of center (importance). For a

given posterior distribution of β , the optimal seed set is $\tilde{\mathbf{x}} = \arg \max_{\mathbf{x}, \sum_j x_j = k} f_\beta(\mathbf{x})$ where

$$\tilde{x}_j = \begin{cases} 1, & \hat{\beta}_j \geq \tilde{\beta}_{(k)} \\ 0, & \text{otherwise} \end{cases} \quad (7)$$

where $\hat{\beta}_j$ is the posterior median of β_j , and $\tilde{\beta}_{(k)}$ is k th order statistic of the posterior medians of β_j for $j \in \{1, \dots, n\}$. After solving for $\tilde{\mathbf{x}}$, we append it and $f(\tilde{\mathbf{x}})$ to \mathbf{X} and \mathbf{y} , respectively, and re-fit the GP regression model to update the posterior distribution of β . This step is repeated B times. Then the optimal seed set is $\mathbf{x}^* = \arg \max_{\mathbf{x} \in \{\mathbf{x}_1, \dots, \mathbf{x}_{N_0+B}\}} f(\mathbf{x})$ where this maximum is taken over the $N_0 + B$ sampled points.

The steps for the entire algorithm are outlined in Algorithm 1. For a given network \mathcal{G} , diffusion mechanism, seed size k , budget N_0, B and shrinkage prior \mathcal{SP} , the algorithm outputs the optimal seed set to maximize the influence spread on \mathcal{G} . We call the method BOPIM for Bayesian OPTimization for Influence Maximization on temporal networks.

Algorithm 1 Bayesian optimization for influence maximization: BOPIM

Result: Optimal seed set S

Input: Objective function $f(\mathbf{x})$; temporal network \mathcal{G} ; seed set size k ; budget B ; number of initial samples N_0 ; shrinkage prior \mathcal{SP}

for N_0 times **do**

 Sample \mathbf{x}_i proportional to node's aggregate degree

 Evaluate $y_i = f(\mathbf{x}_i)$

end

Compute posterior of β using \mathcal{SP}

for B times **do**

 Find $\tilde{\mathbf{x}} = \arg \max_{\mathbf{x}, \sum_j x_j = k} f_\beta(\mathbf{x})$ using (7)

 Compute $y = f(\tilde{\mathbf{x}})$

 Append observation and re-compute posterior of β using \mathcal{SP}

end

return $\mathbf{x}^* = \arg \max_{\mathbf{x} \in \{\mathbf{x}_1, \dots, \mathbf{x}_{N_0+B}\}} f(\mathbf{x})$

2.4 Discussion

Finding the optimal seed set for IM on temporal networks is a constrained, combinatorial optimization problem. To the knowledge of the author, BOPIM is the first application of BO to such a setting. The challenges associated with constrained optimization are mitigated with our simple surrogate function (3) that is linear in the marginal contribution of each node to the influence spread. This model implicitly assumes that there is no interaction between nodes in the seed set. From previous studies on IM, we know that this is not the case as there can be large overlap in the influence of a particular node. This approximation, however, is analogous to the individual-node mean-field approximation [39] used in [16], and in practice, we found that this simple model performs well, and the simplicity makes it straightforward to maximize.

BOPIM is much faster than a standard greedy approach since the costly objective function $f(\cdot)$ only needs to be evaluated $N_0 + B$ times, as opposed to $O(nk)$ times for a greedy algorithm. The run-time is also effectively independent of

the size of the seed set k . Moreover, it is trivial to adapt the algorithm to other diffusion mechanisms as the influence spread function is treated as a black-box in BOPIM.

In addition to its efficiency, BOPIM allows for uncertainty quantification (UQ) of the total influence spread, $\sigma(S)$, and seed set, S . By evaluating a given seed set using the posterior distribution of β , we obtain a complete posterior predictive distribution for the total influence spread. This is in contrast with node-ranking heuristics, which do not yield an estimated influence spread, and probabilistic approximations, which yield a point estimate but not a measure of uncertainty of the total spread. Moreover, if a researcher wants to estimate the expected influence spread for another seed set $S' \neq S$, then the entire calculation needs to be re-run for previous methods. After BOPIM has been fit once, the influence spread for any seed set can be estimated immediately. Please see Section 3.4 for a full discussion of UQ in the seed sets.

Finally, there are several hyper-parameters that need to be chosen for BOPIM. For the number of initial samples N_0 , if this value is large, then the surrogate function will fit the true function well, but at a high computational cost. We found that setting $N_0 = 20$ led to a good balance of fit and speed. Additionally, increasing the budget B led to minimal gains, so we recommend setting this to be fairly small at $B = 5$. For computing the posterior of β , the number of MCMC samples also must be selected. Again, more MCMC samples lead to better estimates of the posterior distribution but also longer run-times. Since we only use the median of the posterior distribution, we can keep the number of MCMC samples relatively small to increase speed. We recommend 6,000 iterations with the first 1,000 used for burn-in. For hyper-parameters in the shrinkage priors, we simply use the default settings from the original papers. Lastly, for the number of MC simulations for the objective function calculation, it is important that this output is accurate so we recommend 1,000 iterations. Unless otherwise noted, use these settings for all experiments in Section 3.

3 EXPERIMENTS

We now study the performance of the proposed method with numerical experiments. All experiments were performed in Python and the code for Algorithm 1 is available on GitHub: <https://github.com/eyanchenko/BOPIM>.

3.1 Data

The following experiments are conducted on four real-world networks. Reality ($n = 64, m = 722$) [40], Hospital ($n = 75, m = 1139$) [41] and High School 1 ($n = 312, m = 2242$) [42] are proximity networks where an edge exists if two people are close to each other. Email 4 ($n = 167, m = 3250$) [43] is a communication network where users share an edge if they email one another. Each network is aggregated into T temporal snapshots of equal duration. We note that these networks are relatively small due to the slow speed of the greedy algorithm. Therefore, in the Supplemental Materials, we conduct experiments using the proposed method on networks with $n = 1899$ [44] and $n = 3188$ [45] nodes to demonstrate its scalability.

3.2 Surrogate function validation

3.2.1 Settings

In the first set of simulations, we quantify the fit of the surrogate model $f_\beta(\cdot)$ in (3) to the true objective function $f(\cdot)$. Towards this end, we first run Algorithm 1 with $N_0 = 20$ and $B = 5$ and save the final posterior distribution of β . Using this posterior distribution, we then compute out-of-sample influence spread predictions on $N = 100$ seed sets and compare with the values of the true objective function. If the surrogate model fits well, then $|f_\beta(x) - f(x)|$ will be small. We quantify this difference using three metrics: mean absolute prediction error (MAPE) and 95% prediction interval coverage and width. If $\hat{\beta}$ is the posterior median, then $\hat{y}_i = f_{\hat{\beta}}(x_i)$ is the posterior median prediction for y_i , and the MAPE is

$$\frac{1}{N} \sum_{i=1}^N |\hat{y}_i - y_i|$$

where N is the number of out-of-sample seed sets. A smaller MAPE means a closer fit. We also compute the 95% prediction interval for each sample and compute the nominal frequentist coverage:

$$\frac{1}{N} \sum_{i=1}^N \mathbb{I}\{y_i \in (\hat{y}_{i,0.025}, \hat{y}_{i,0.975})\}$$

where $\mathbb{I}(\cdot)$ is the indicator function and $\hat{y}_{i,\alpha}$ is the α percentile prediction for y_i . While there is no guarantee that a Bayesian framework yields nominal frequentist coverage, it is still a useful metric of comparison. Lastly, we compute the 95% prediction interval width as $(\hat{y}_{i,0.975} - \hat{y}_{i,0.025})$ where a smaller width means a more precise estimate.

We compute these statistics for each shrinkage prior on each of the four data sets. We fix $\lambda = 0.05$, and $k = 3, 4, 8, 15$ for the Reality, Hospital, Email 4 and High School 1 datasets, respectively. k was chosen as approximately 5% of the total number of nodes for each network. For the out-of-sample predictions, we consider two node sampling schemes. One samples nodes at random while the other samples according to their degree on the aggregate network, as in BOPIM. We expect the model to have a closer fit when the test points are sampled in the same way as the training points.

3.2.2 Results

The results are in Table 1. Note that the MAPE results are interpreted as follows: for the Reality network and R2D2 prior with degree-based sampling of seed sets, for example, the MAPE value of 2.44 means that, on average, the estimated influence spread of the surrogate function (3) is within about two nodes of the true influence spread. Now, for this network, the R2D2 prior leads to the lowest MAPE for Degree-based sampling of the test points, while all priors are comparable for random sampling. The R2D2 prior also leads to significantly narrower credible intervals than that of DL and HS, but also the lowest coverage rate. HS has the best coverage and largest width. The MAPE value is lower when the out-of-sample test points are sampled proportionally to degree for the R2D2 prior, but are similar across sampling methods for the DL and HS priors.

The results for Hospital, Email 4 and High School 1 are similar. In each data set, all methods have comparable

MAPE values. The HS prior has the highest coverage, as well as the widest credible intervals, while the R2D2 prior leads to the narrowest credible intervals and lowest coverage. In each setting, the MAPE values are larger when the test points are sampled randomly. Thus, the surrogate model fits the true objective function more closely when the seed nodes have a large degree, which is where we hypothesize that the global optimum lies.

3.3 Influence maximization

For the second set of experiments, we compare the method’s performance on the IM task.

3.3.1 Settings

We simulate the influence diffusion process and select seed sets for IM using BOPIM. The main metrics of comparison are the number of influenced nodes at the conclusion of the spreading process, and the total algorithmic run time. We compare BOPIM with a greedy algorithm as this is considered the “gold standard” in IM. [46] proved that the SI model of diffusion is monotone and sub-modular so we use the CELF [47] step to increase the speed of the greedy algorithm. All experiments are conducted under the *ex post* assumption where the future evolution of the network is known when selecting seed nodes as in [6], [14], [15], [16]. While this assumption may be unrealistic in some cases, the main goal of this work is to propose a BO scheme for IM rather than tackling the *ex ante* problem [48]. We leave this as an important avenue of future work. Finally, to compare the different methods, we vary the number of seed nodes (k), number of snapshots (T), and infection parameter (λ).

3.3.2 Results

First, we fix $\lambda = 0.05$ and $T = 10$ and vary k . For this setting, we record both the influence spread and computing time with the results in Figures 1 and 7. For each data set, the proposed BO method yields comparable influence spread to the greedy algorithm. For Reality and Hospital, in particular, the spreads are almost indistinguishable between the different methods. The greedy algorithm performs slightly better in Email 4 and High School 1 but the proposed method is still comparable. Additionally, there is no clear trend on which shrinkage prior is superior as each yields similar influence spreads. In terms of computing time, the proposed method has a large advantage over the greedy algorithm. In each case, the computational time increases with k for the greedy algorithm, whereas that of the proposed method is relatively constant across seed sizes. For large k , the proposed method is between five (Reality) and seventeen (High School 1) times faster than the greedy algorithm. The HS prior is also consistently faster than both DL and R2D2.

Next we fix k such that roughly 5% of the total number of nodes are initially activated and $\lambda = 0.05$. We vary the number of aggregations of the temporal network, where small and large T correspond to granular and fine aggregations, respectively. The results are in Figure 3. The trends are similar to that of varying k . Across networks and T , the proposed method yields comparable influence spread to that of the greedy algorithm and there is again no clear difference between the different shrinkage priors. Note that

the total spread increases with T as there are more rounds for influence to diffuse.

Finally, we fix k at 5% of n and $T = 10$ and vary the infection probability λ . The results are in Figure 4 and are similar for each network: as λ increases, the total influence spread also increases and the influence spreads are comparable for the greedy algorithm and different shrinkage priors.

3.4 Uncertainty quantification

The proposed method also provides a measure of uncertainty for the optimal seed sets. Uncertainty quantification (UQ) is useful for a richer understanding of the outputted solution and can answer questions such as: Are there many seed sets which yield near optimal spread? Can the selection of seed nodes be viewed on a spectrum as opposed to binary inclusion/exclusion? We take a first step towards answering these questions with the proposed method.

Recall that we use GP regression to model the objective function. In (3), β_i corresponds to the inclusion ($x_i = 1$) or exclusion ($x_i = 0$) of node i in the seed set, and we obtain the complete posterior distribution for each coefficient. For the acquisition function step of BOPIM, we only use the median of this posterior distribution to rank nodes by influence. We can leverage the entire distribution, however, to obtain a richer understanding of a node’s importance.

To do this, we save the final posterior distribution of β in BOPIM for the Reality network with $k = 5$, $T = 10$, $\lambda = 0.05$ and the DL prior (15,000 MCMC samples, 5,000 burn-in). The results for the HS and R2D2 priors are in the Supplemental Materials. In Figure 9a, we report the box-plot for the posterior distribution of β_i for each node $i \in \{1, \dots, n\}$. The largest posterior distributions correspond with the ideal nodes for the seed set. From the figure, nodes 1, 7 and 27 have noticeably larger values of the posterior distribution than that of the other nodes. Thus, while the the k nodes with largest posterior median are chosen for the seed set, it is clear that nodes 1, 7 and 27 are noticeably more influential than the other two nodes included in the seed set (12 and 54).

In Figure 9b, we plot the proportion of MCMC samples for which the coefficient estimate is in the top k of all nodes. This plot shows the proportion of MCMC iterations for which a node would be included in the seed set. For example, node 1’s coefficient estimate was in the top k of all nodes in 100% of the MCMC samples, thus making it the most influential node. While nodes 1, 7, 12 and 27 have noticeably larger proportions than all other nodes, the fifth largest (54) has a comparable proportion to nodes 8 and 58. Thus, it is likely that there are several choices for the fifth node in the seed set that would lead to similar influence spreads.

4 DISCUSSION AND CONCLUSION

In this work, we apply a Bayesian Optimization framework to solve the influence maximization problem on temporal networks. The proposed BOPIM algorithm models the influence spread function via Gaussian Process regression and shrinkage priors, and uses the posterior median to

Dataset	Sampling	Prior	MAPE	Coverage	Width
Reality	Random	HS	3.28 (0.22)	0.99	29.15
		DL	3.12 (0.22)	0.33	3.53
		R2D2	3.45 (0.23)	0.10	0.72
	Degree	HS	3.33 (0.22)	1.00	20.80
		DL	3.27 (0.21)	0.46	5.37
		R2D2	2.44 (0.18)	0.11	0.85
Hospital	Random	HS	4.32 (0.42)	0.90	18.38
		DL	3.99 (0.39)	0.34	4.43
		R2D2	4.02 (0.41)	0.04	0.40
	Degree	HS	3.21 (0.30)	1.00	20.45
		DL	3.44 (0.31)	0.43	4.08
		R2D2	3.73 (0.31)	0.03	0.42
Email 4	Random	HS	1.32 (0.19)	0.97	10.12
		DL	1.24 (0.19)	0.55	2.17
		R2D2	1.32 (0.19)	0.13	0.51
	Degree	HS	1.26 (0.09)	0.91	5.34
		DL	1.25 (0.10)	0.42	1.76
		R2D2	1.27 (0.09)	0.08	0.25
High School 1	Random	HS	7.41 (0.43)	1.00	> 100
		DL	7.52 (0.44)	0.08	3.23
		R2D2	7.57 (0.42)	0.01	0.19
	Degree	HS	3.32 (0.24)	1.00	> 100
		DL	4.05 (0.27)	0.19	3.23
		R2D2	3.33 (0.23)	0.02	0.25

Table 1: Results on validating surrogate function. Standard error in parentheses. The best mean absolute prediction errors (MAPE) are in **bold**.

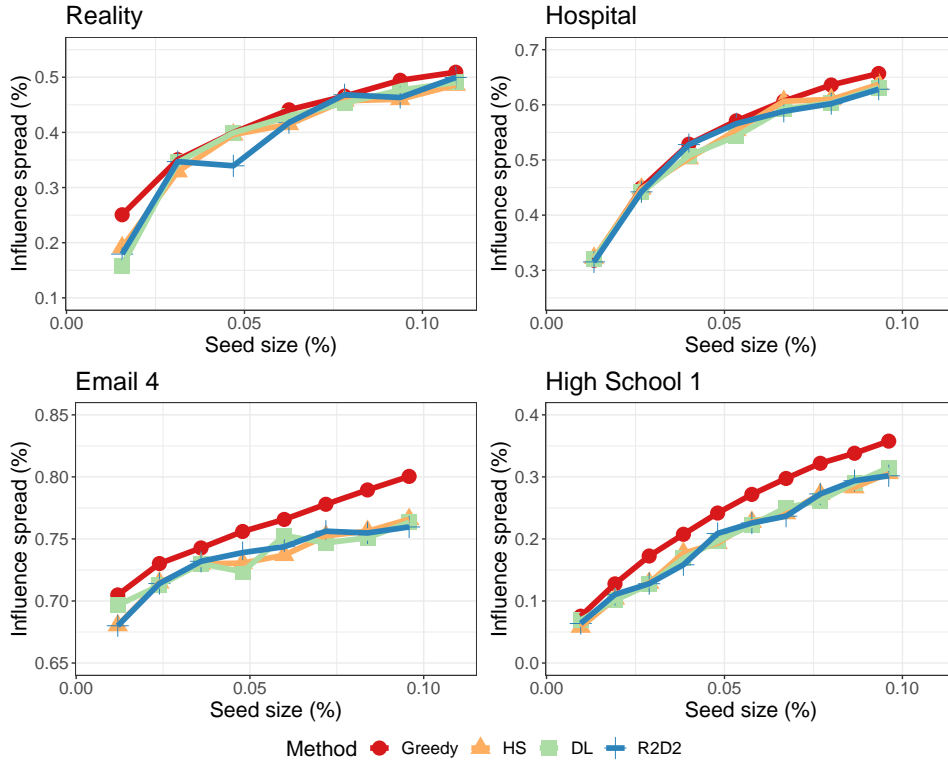


Figure 1: Influence spread results for increasing seed size (k).

approximate the global optimum. Experiments showed that despite being such a simple surrogate, the statistical model’s estimated influence spread is, on average, within a few

nodes to the true spread. In the IM simulations, the proposed method yields influence spreads comparable to that of seed sets from a greedy algorithm. The BO approach,

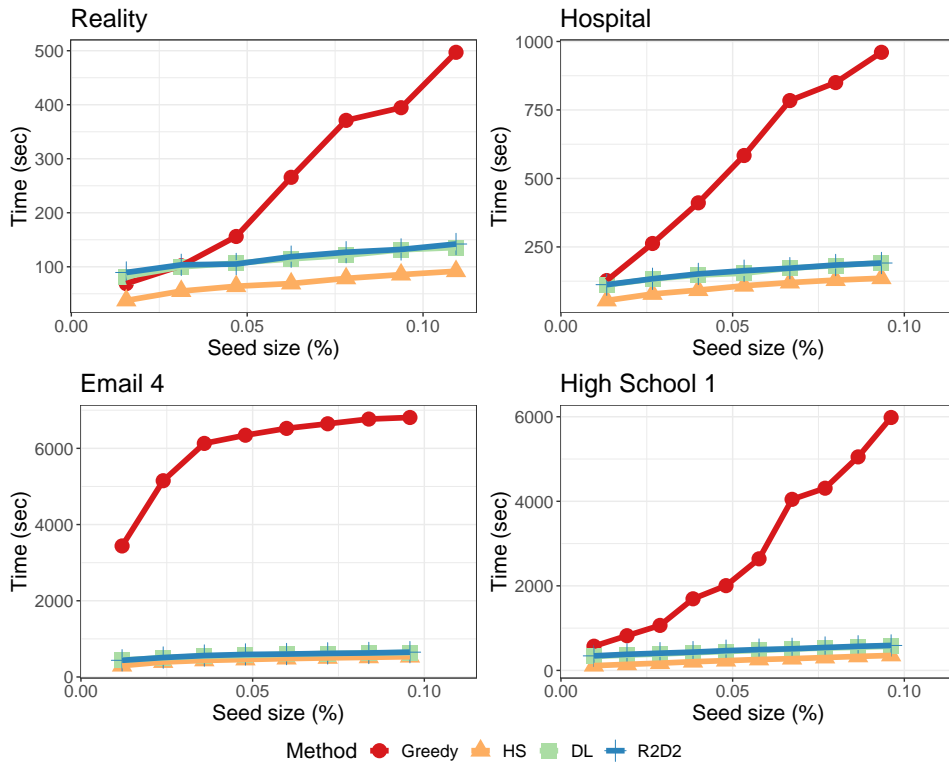


Figure 2: Computation time results for increasing seed size (k).

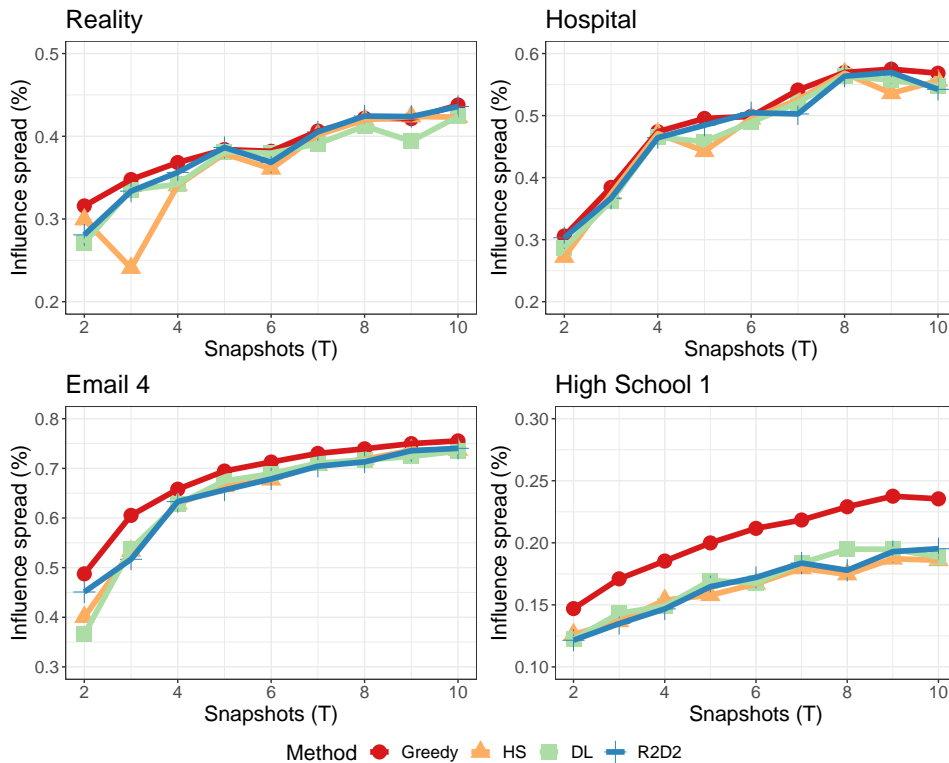


Figure 3: Influence spread results for increasing number of snapshots (T).

however, is as much as seventeen times faster than the greedy algorithm. The UQ found evidence that there are many seed sets which yield comparably optimal influence spread, thus implying that the objective function is relatively

“flat.” Finally, we remark that both the DL and R2D2 priors were slightly slower than the HS prior in IM simulations due to the fact that both of these methods sample from the generalized inverse Gaussian distribution, which does not

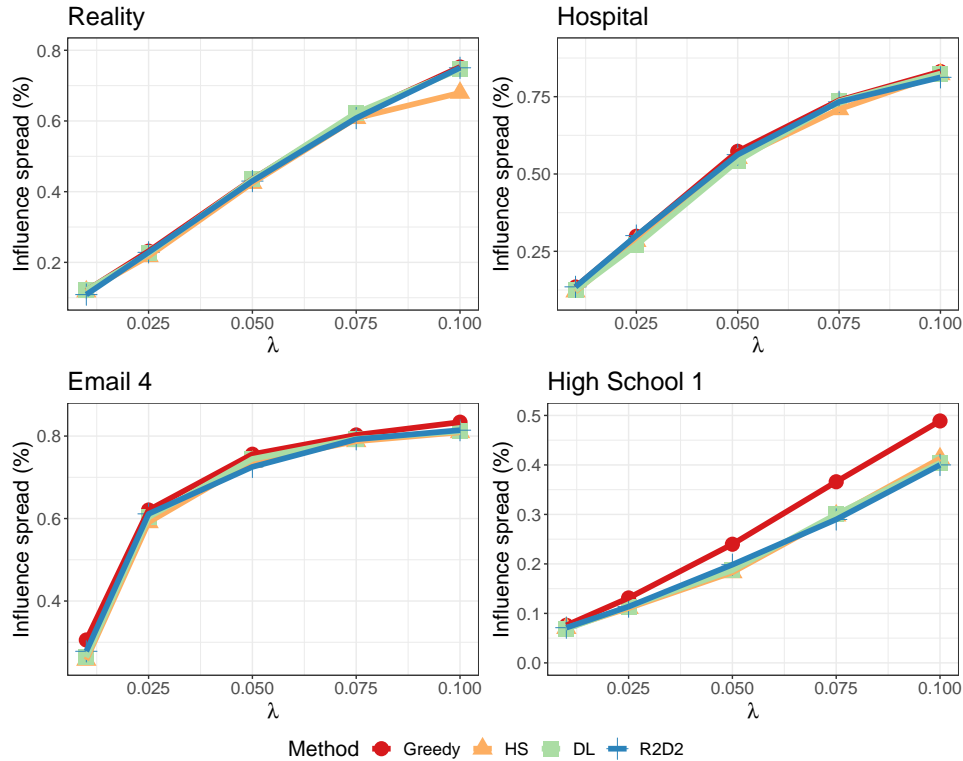


Figure 4: Influence spread results for increasing infection probability (λ).

have an optimized sampler in Python.

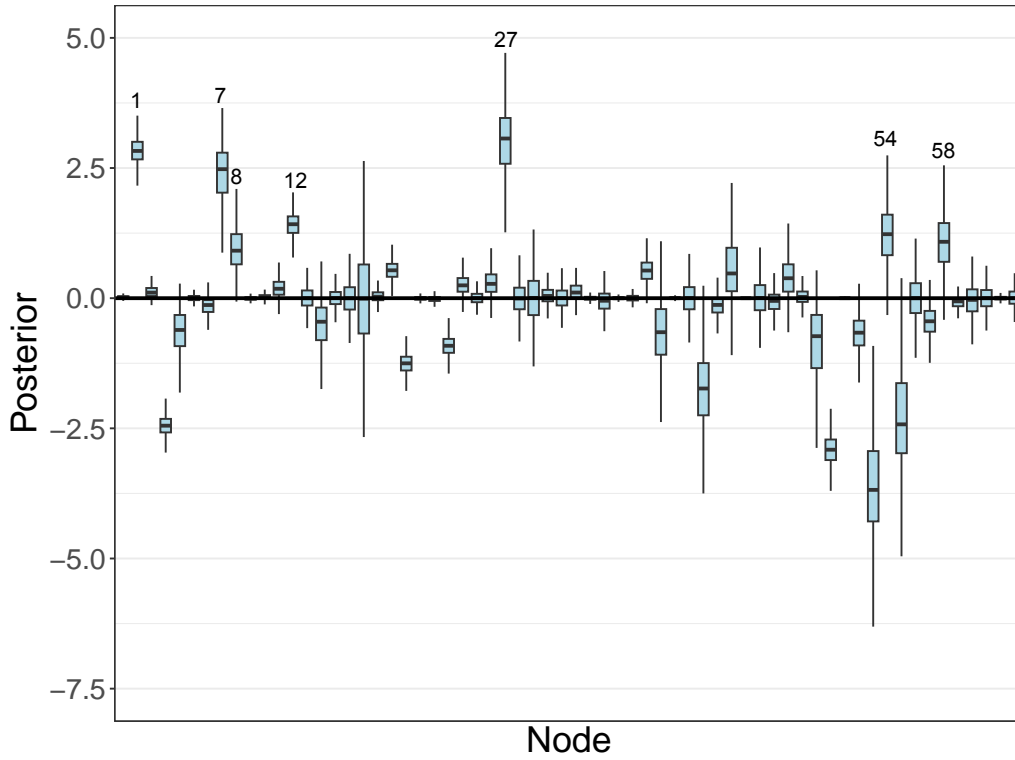
There are many interesting avenues to extend this work. First, we could study the performance of the proposed method when the model is fit using a particular k , but the final seed set has $k' \neq k$ seed nodes. If this still leads to good performance then it would demonstrate greater flexibility of the method. Another area of extension is considering more complicated surrogate functions that take into account interactions between nodes in the seed set [32]. This should lead to better performance that may even exceed the greedy algorithm. However, the number of parameters in the model would be $O(n^2)$ and the acquisition function step would also be much more challenging. Considering the *ex ante* IM task is another important open-problem.

ACKNOWLEDGMENTS

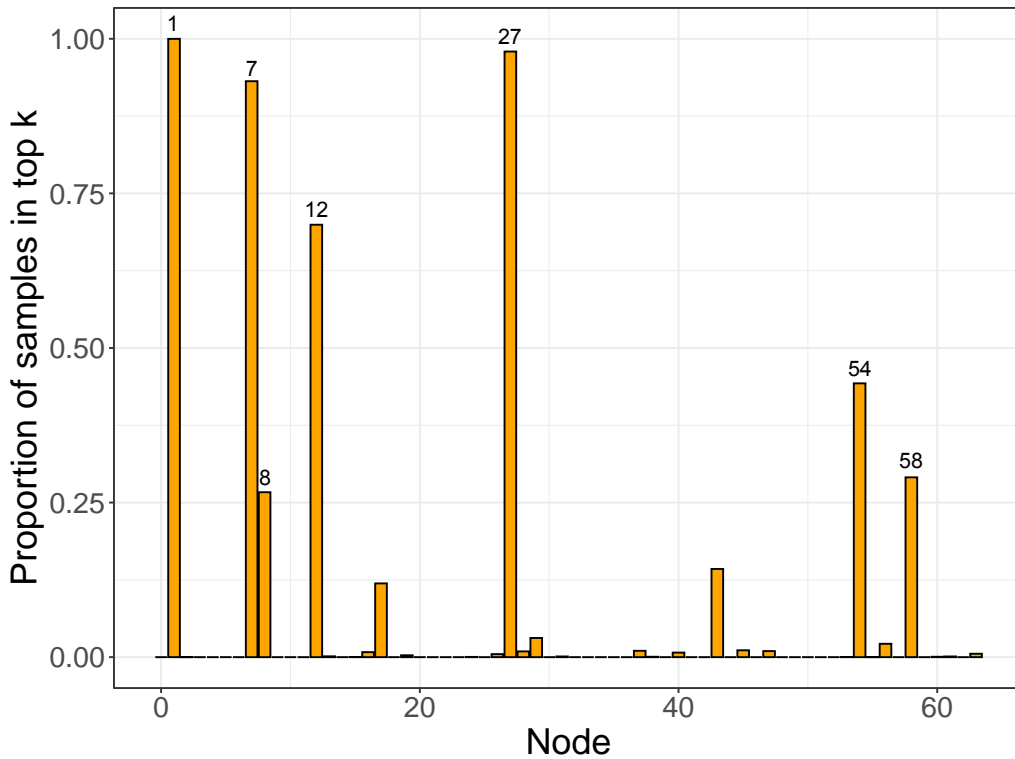
This work was conducted while EY was on a JSPS Pre-doctoral Fellowship for Research in Japan (Short-term Program).

REFERENCES

- [1] D. Kempe, J. Kleinberg, and É. Tardos, "Maximizing the spread of influence through a social network," in *Proceedings of the 9th ACM SIGKDD International Conference on Knowledge Discovery and Data Mining*, 2003, pp. 137–146.
- [2] W. Chen, Y. Wang, and S. Yang, "Efficient influence maximization in social networks," in *Proceedings of the 15th ACM SIGKDD International Conference on Knowledge Discovery and Data Mining*, 2009, pp. 199–208.
- [3] P. Domingos and M. Richardson, "Mining the network value of customers," in *Proceedings of the seventh ACM SIGKDD international conference on Knowledge discovery and data mining*, 2001, pp. 57–66.
- [4] S. Bharathi, D. Kempe, and M. Salek, "Competitive influence maximization in social networks," in *Internet and Network Economics: Third International Workshop, WINE 2007, San Diego, CA, USA, December 12-14, 2007. Proceedings 3*. Springer, 2007, pp. 306–311.
- [5] W. Chen, Y. Yuan, and L. Zhang, "Scalable influence maximization in social networks under the linear threshold model," in *2010 IEEE International Conference on Data Mining*. IEEE, 2010, pp. 88–97.
- [6] T. Murata and H. Koga, "Extended methods for influence maximization in dynamic networks," *Computational Social Networks*, vol. 5, no. 1, pp. 1–21, 2018.
- [7] B. Wilder, A. Yadav, N. Immerlica, E. Rice, and M. Tambe, "Uncharted but not uninfluenced: Influence maximization with an uncertain network," in *Proceedings of the 16th Conference on Autonomous Agents and MultiAgent Systems*, 2017, pp. 1305–1313.
- [8] A. Yadav, B. Wilder, E. Rice, R. Petering, J. Craddock, A. Yoshioka-Maxwell, M. Hemler, L. Onasch-Vera, M. Tambe, and D. Woo, "Influence maximization in the field: The arduous journey from emerging to deployed application," in *Proceedings of the 16th conference on autonomous agents and multiagent systems*, 2017, pp. 150–158.
- [9] B. Wilder, L. Onasch-Vera, J. Hudson, J. Luna, N. Wilson, R. Petering, D. Woo, M. Tambe, and E. Rice, "End-to-end influence maximization in the field," in *AAMAS*, vol. 18, 2018, pp. 1414–1422.
- [10] A. Yadav, B. Wilder, E. Rice, R. Petering, J. Craddock, A. Yoshioka-Maxwell, M. Hemler, L. Onasch-Vera, M. Tambe, and D. Woo, "Bridging the gap between theory and practice in influence maximization: Raising awareness about hiv among homeless youth," in *IJCAI*, 2018, pp. 5399–5403.
- [11] P. Holme, "Efficient local strategies for vaccination and network attack," *Europhysics Letters*, vol. 68, no. 6, p. 908, 2004.
- [12] S. Lee, L. E. C. Rocha, F. Liljeros, and P. Holme, "Exploiting temporal network structures of human interaction to effectively immunize populations," *PLOS ONE*, vol. 7, no. 5, p. 0036439, 05 2012.
- [13] P. Holme and J. Saramäki, "Temporal networks," *Physics Reports*, vol. 519, no. 3, pp. 97–125, 2012.
- [14] C. C. Aggarwal, S. Lin, and P. S. Yu, "On influential node discovery in dynamic social networks," in *Proceedings of the 2012 SIAM International Conference on Data Mining*. SIAM, 2012, pp. 636–647.



(a) Posterior distribution box plots.



(b) Proportion of MCMC samples in top k .

Figure 5: Posterior distribution summaries for Dirichlet-Laplace prior and Reality network.

[15] S. Osawa and T. Murata, "Selecting seed nodes for influence maximization in dynamic networks," in *Complex Networks VI*, G. Mangioni, F. Simini, S. M. Uzzo, and D. Wang, Eds. Springer, 2015, pp. 91–98.

[16] Ş. Erkol, D. Mazzilli, and F. Radicchi, "Influence maximization on

temporal networks," *Physical Review E*, vol. 102, no. 4, p. 042307, 2020.

[17] R. Michalski, T. Kajdanowicz, P. Bródka, and P. Kazienko, "Seed selection for spread of influence in social networks: Temporal vs. static approach," *New Generation Computing*, vol. 32, no. 3, pp. 213–

- 235, 2014.
- [18] R. Michalski, J. Jankowski, and P. Pazura, "Entropy-based measure for influence maximization in temporal networks," in *Computational Science—ICCS 2020: 20th International Conference, Amsterdam, The Netherlands, June 3–5, 2020, Proceedings, Part IV 20*. Springer, 2020, pp. 277–290.
- [19] E. Yanchenko, T. Murata, and P. Holme, "Influence maximization on temporal networks: a review," *arXiv preprint arXiv:2307.00181*, 2023.
- [20] J. Snoek, H. Larochelle, and R. P. Adams, "Practical bayesian optimization of machine learning algorithms," *Advances in neural information processing systems*, vol. 25, 2012.
- [21] B. Shahriari, K. Swersky, Z. Wang, R. P. Adams, and N. De Freitas, "Taking the human out of the loop: A review of bayesian optimization," *Proceedings of the IEEE*, vol. 104, no. 1, pp. 148–175, 2015.
- [22] P. I. Frazier, "A tutorial on bayesian optimization," *arXiv preprint arXiv:1807.02811*, 2018.
- [23] J. Wu, X.-Y. Chen, H. Zhang, L.-D. Xiong, H. Lei, and S.-H. Deng, "Hyperparameter optimization for machine learning models based on bayesian optimization," *Journal of Electronic Science and Technology*, vol. 17, no. 1, pp. 26–40, 2019.
- [24] R. Turner, D. Eriksson, M. McCourt, J. Kiili, E. Laaksonen, Z. Xu, and I. Guyon, "Bayesian optimization is superior to random search for machine learning hyperparameter tuning: Analysis of the black-box optimization challenge 2020," in *NeurIPS 2020 Competition and Demonstration Track*. PMLR, 2021, pp. 3–26.
- [25] P. I. Frazier and J. Wang, "Bayesian optimization for materials design," in *Information science for materials discovery and design*. Springer, 2015, pp. 45–75.
- [26] S. Greenhill, S. Rana, S. Gupta, P. Vellanki, and S. Venkatesh, "Bayesian optimization for adaptive experimental design: A review," *IEEE access*, vol. 8, pp. 13 937–13 948, 2020.
- [27] C. Wang, W. Chen, and Y. Wang, "Scalable influence maximization for independent cascade model in large-scale social networks," *Data Mining and Knowledge Discovery*, vol. 25, pp. 545–576, 2012.
- [28] Z. Wen, B. Kveton, M. Valko, and S. Vaswani, "Online influence maximization under independent cascade model with semi-bandit feedback," *Advances in Neural Information Processing Systems*, vol. 30, 2017.
- [29] W. Chen, C. Wang, and Y. Wang, "Scalable influence maximization for prevalent viral marketing in large-scale social networks," in *Proceedings of the 16th ACM SIGKDD International Conference on Knowledge Discovery and Data Mining*, 2010, pp. 1029–1038.
- [30] A. Goyal, W. Lu, and L. V. Lakshmanan, "Celf++ optimizing the greedy algorithm for influence maximization in social networks," in *Proceedings of the 20th International Conference Companion on World Wide Web*, 2011, pp. 47–48.
- [31] Y. Li, J. Fan, Y. Wang, and K.-L. Tan, "Influence maximization on social graphs: A survey," *IEEE Transactions on Knowledge and Data Engineering*, vol. 30, no. 10, pp. 1852–1872, 2018.
- [32] R. Baptista and M. Poloczek, "Bayesian optimization of combinatorial structures," in *International Conference on Machine Learning*. PMLR, 2018, pp. 462–471.
- [33] C. M. Carvalho, N. G. Polson, and J. G. Scott, "Handling sparsity via the horseshoe," in *Artificial intelligence and statistics*. PMLR, 2009, pp. 73–80.
- [34] —, "The horseshoe estimator for sparse signals," *Biometrika*, vol. 97, no. 2, pp. 465–480, 2010.
- [35] E. Makalic and D. F. Schmidt, "A simple sampler for the horseshoe estimator," *IEEE Signal Processing Letters*, vol. 23, no. 1, pp. 179–182, 2015.
- [36] A. Bhattacharya, D. Pati, N. S. Pillai, and D. B. Dunson, "Dirichlet-laplace priors for optimal shrinkage," *Journal of the American Statistical Association*, vol. 110, no. 512, pp. 1479–1490, 2015.
- [37] Y. D. Zhang, B. P. Naughton, H. D. Bondell, and B. J. Reich, "Bayesian regression using a prior on the model fit: The r2-d2 shrinkage prior," *Journal of the American Statistical Association*, vol. 117, no. 538, pp. 862–874, 2022.
- [38] E. Yanchenko, H. D. Bondell, and B. J. Reich, "The r2d2 prior for generalized linear mixed models," *arXiv preprint arXiv:2111.10718*, 2021.
- [39] R. Pastor-Satorras, C. Castellano, P. Van Mieghem, and A. Vespignani, "Epidemic processes in complex networks," *Reviews of modern physics*, vol. 87, no. 3, p. 925, 2015.
- [40] N. Eagle and A. Pentland, "Reality mining: sensing complex social systems," *Personal and Ubiquitous Computing*, vol. 10, pp. 255–268, 2006.
- [41] P. Vanhems, A. Barrat, C. Cattuto, J.-F. Pinton, N. Khanafer, C. Régis, B.-a. Kim, B. Comte, and N. Voirin, "Estimating potential infection transmission routes in hospital wards using wearable proximity sensors," *PloS one*, vol. 8, no. 9, p. e73970, 2013.
- [42] R. Mastrandrea, J. Fournet, and A. Barrat, "Contact patterns in a high school: a comparison between data collected using wearable sensors, contact diaries and friendship surveys," *PLOS One*, vol. 10, no. 9, p. e0136497, 2015.
- [43] R. Michalski, S. Palus, and P. Kazienko, "Matching organizational structure and social network extracted from email communication," in *Business Information Systems: 14th International Conference, BIS 2011, Poznań, Poland, June 15–17, 2011. Proceedings 14*. Springer, 2011, pp. 197–206.
- [44] P. Panzarasa, T. Opsahl, and K. M. Carley, "Patterns and dynamics of users' behavior and interaction: Network analysis of an online community," *Journal of the American Society for Information Science and Technology*, vol. 60, no. 5, pp. 911–932, 2009.
- [45] J.-P. Eckmann, E. Moses, and D. Sergi, "Entropy of dialogues creates coherent structures in e-mail traffic," *Proceedings of the National Academy of Sciences*, vol. 101, no. 40, pp. 14 333–14 337, 2004.
- [46] Ş. Erkol, D. Mazzilli, and F. Radicchi, "Effective submodularity of influence maximization on temporal networks," *Physical Review E*, vol. 106, no. 3, p. 034301, 2022.
- [47] J. Leskovec, A. Krause, C. Guestrin, C. Faloutsos, J. VanBriesen, and N. Glance, "Cost-effective outbreak detection in networks," in *Proceedings of the 13th ACM SIGKDD International Conference on Knowledge Discovery and Data Mining*, 2007, pp. 420–429.
- [48] E. Yanchenko, T. Murata, and P. Holme, "Link prediction for ex ante influence maximization on temporal networks," *arXiv preprint arXiv:2305.09965*, 2023.
- [49] N. G. Polson and J. G. Scott, "Shrink globally, act locally: Sparse bayesian regularization and prediction," *Bayesian statistics*, vol. 9, no. 501–538, p. 105, 2010.
- [50] Y. Zhang and H. D. Bondell, "Variable selection via penalized credible regions with dirichlet-laplace global-local shrinkage priors," *Bayesian Analysis*, vol. 13 (3), pp. 823–844, 2018.



Eric Yanchenko received a BS in Mathematics and Physics from The Ohio State University, Columbus, Ohio, USA. He is currently a PhD candidate in Statistics at North Carolina State University, Raleigh, North Carolina, USA and a Japan Society for Promotion of Science (JSPS) Short-term Fellow at Tokyo Institute of Technology, Tokyo, Japan. His research interests include hypothesis testing for meso-scale structures on graphs, eliciting prior distributions for scale parameters in hierarchical Bayesian models, and

influence maximization.

5 SUPPLEMENTAL MATERIALS

5.1 Gibbs samplers

In this section, we report the Gibbs samplers for each of the three shrinkage priors.

5.1.1 Horseshoe prior

For the Horseshoe prior [49], we use the auxiliary variable formulation of [35].

- 1) Sample $\beta|\lambda, \nu, \tau^2, \sigma^2, \mathbf{Y} \sim \mathbf{N}(\boldsymbol{\mu}, \sigma^2 \mathbf{V})$ where $\boldsymbol{\mu} = \mathbf{V}\mathbf{X}^T\mathbf{Y}$, $V = (\mathbf{X}^T\mathbf{X} + \mathbf{S}^{-1})^{-1}$, $\mathbf{S} = \text{diag}(\lambda_1^2\tau^2, \dots, \lambda_n^2\tau^2)$.
- 2) Sample $\sigma^2|\beta, \lambda, \nu, \tau^2, \mathbf{Y} \sim \text{IG}(a_1 + (N_0 + n)/2, b_1 + (\beta^T\mathbf{S}^{-1}\beta + (\mathbf{Y} - \mathbf{X}\beta)^T(\mathbf{Y} - \mathbf{X}\beta))/2)$.
- 3) Sample $\lambda_j^2|\beta, \nu, \tau^2, \sigma^2 \sim \text{IG}(1, \nu_j^{-1} + \beta_j^2/(2\tau^2\sigma^2))$, $j = 1, \dots, n$.
- 4) Sample $\tau^2|\beta, \lambda, \sigma^2, \xi \sim \text{IG}((n + 1)/2, \xi^{-1} + \sum_{k=1}^n \beta_k^2/(2\lambda_k^2\sigma^2))$.
- 5) Sample $\nu_j|\lambda_k \sim \text{IG}(1, 1 + \lambda_j^{-2})$ for $j = 1, \dots, n$.
- 6) Sample $\xi|\tau^2 \sim \text{IG}(1, 1 + \tau^{-2})$.

5.1.2 Dirichlet-Laplace prior

For the Dirichlet-Laplace prior, we use the Gibbs sampler from [50]. Additionally, if $Z \sim \text{InvGaussian}(\mu, \lambda)$ then $\pi(z) = \lambda^{1/2}(2\pi z^3)^{-1/2} \exp\{-\lambda(z - \mu)^2/(2\mu^2 z)\}$; and $Z \sim \text{GIG}$, the generalized inverse gaussian distribution, then $\pi(z) \propto z^{-\lambda_0} \exp\{-\rho z + \chi/z\}/2\}$.

- 1) Sample $\beta|\psi, \phi, \tau, \sigma^2, \mathbf{Y} \sim \mathbf{N}(\boldsymbol{\mu}, \sigma^2 \mathbf{V})$ where $\boldsymbol{\mu} = \mathbf{V}\mathbf{X}^T\mathbf{Y}$, $V = (\mathbf{X}^T\mathbf{X} + \mathbf{S}^{-1})^{-1}$, $\mathbf{S} = \text{diag}(\psi_1\phi_1^2\tau^2, \dots, \psi_n\phi_n^2\tau^2)$.
- 2) Sample $\sigma^2|\beta, \psi, \phi, \tau, \mathbf{Y} \sim \text{IG}(a_1 + (N_0 + n)/2, b_1 + (\beta^T\mathbf{S}^{-1}\beta + (\mathbf{Y} - \mathbf{X}\beta)^T(\mathbf{Y} - \mathbf{X}\beta))/2)$.
- 3) Sample $\psi|\beta, \phi, \tau, \sigma^2$. Draw $\psi_j^{-1} \sim \text{InvGaussian}(\mu_j = \sigma\phi_j\tau/|\beta_j|, \lambda = 1)$ and take reciprocal for ψ_j .
- 4) Sample $\tau|\beta, \phi, \sigma^2 \sim \text{GIG}(\chi = 2\sum_{j=1}^N |\beta_j|/(\sigma\phi_j), \rho = 1, \lambda_0 = na - n)$.
- 5) Sample $\phi|\beta, \psi, \xi, \sigma^2$. If $a = na_\pi$, then draw T_1, \dots, T_n independently with $T_j \sim \text{GIG}(\chi = 2|\beta_j|/\sigma, \rho = 1, \lambda_0 = a - 1)$ and set $\phi_j = T_j/\sum_{k=1}^n T_k$.

5.1.3 R2D2 prior

For the R2D2 prior, we use the Gibbs sampler from [37].

- 1) Sample $\beta|\psi, \phi, \omega, \sigma^2, \mathbf{Y} \sim \mathbf{N}(\boldsymbol{\mu}, \sigma^2 \mathbf{V})$ where $\boldsymbol{\mu} = \mathbf{V}\mathbf{X}^T\mathbf{Y}$, $V = (\mathbf{X}^T\mathbf{X} + \mathbf{S}^{-1})^{-1}$, $\mathbf{S} = \text{diag}(\psi_1\phi_1\omega/2, \dots, \psi_n\phi_n\omega/2)$.
- 2) Sample $\sigma^2|\beta, \psi, \phi, \omega, \mathbf{Y} \sim \text{IG}(a_1 + (N_0 + n)/2, b_1 + (\beta^T\mathbf{S}^{-1}\beta + (\mathbf{Y} - \mathbf{X}\beta)^T(\mathbf{Y} - \mathbf{X}\beta))/2)$.
- 3) Sample $\psi|\beta, \phi, \omega, \sigma^2$. Draw $\psi_j^{-1} \sim \text{InvGaussian}(\mu_j = \sqrt{\sigma^2\phi_j\omega/2}/|\beta_j|, \lambda = 1)$ and take reciprocal for ψ_j .
- 4) Sample $\omega|\beta, \psi, \phi, \xi, \sigma^2 \sim \text{GIG}(\chi = \sum_{j=1}^N 2\beta_j^2/(\sigma^2\psi_j\phi_j), \rho = 2\xi, \lambda_0 = a - n/2)$.
- 5) Sample $\xi|\omega \sim \text{Gamma}(a + b, 1 + \omega)$.
- 6) Sample $\phi|\beta, \psi, \xi, \sigma^2$. If $a = na_\pi$, then draw T_1, \dots, T_n independently with $T_j \sim \text{GIG}(\chi = 2\beta_j^2/(\sigma^2\psi_j), \rho = 2\xi, \lambda_0 = a_\pi - 1/2)$ and set $\phi_j = T_j/\sum_{k=1}^n T_k$.

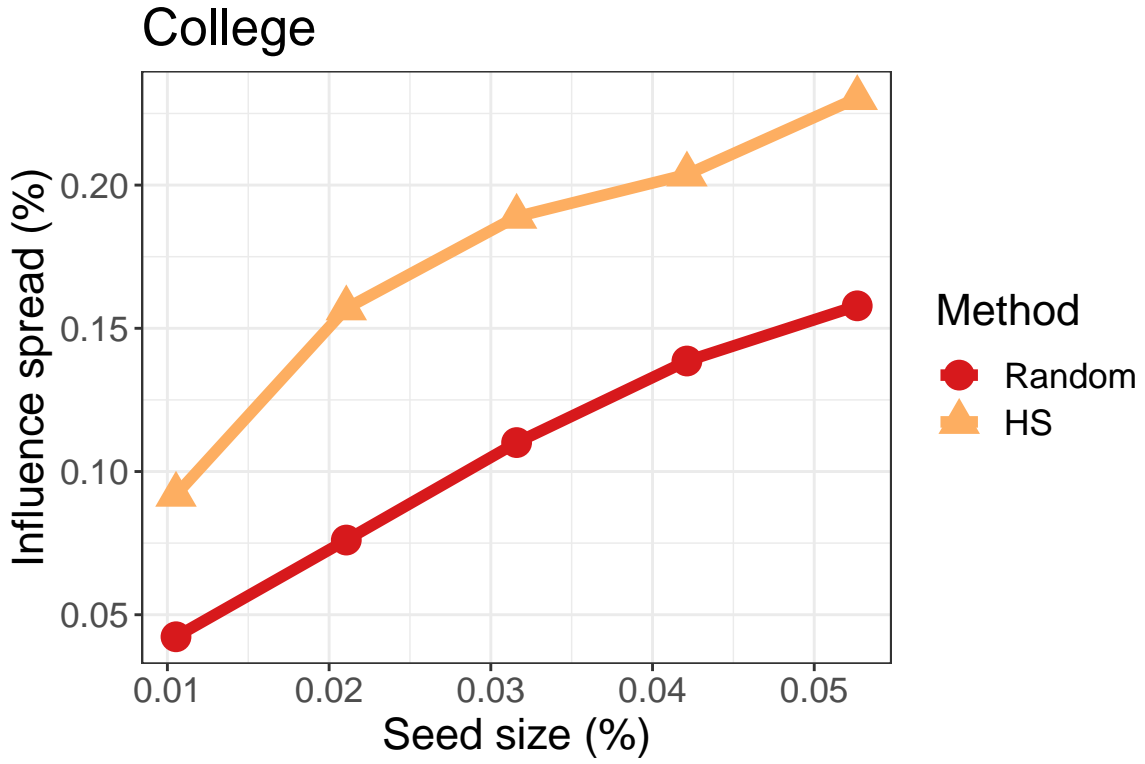
5.2 IM for large networks

To demonstrate the performance of BOPIM on large networks, we present the results for IM on the College network [44] with $n = 1899$, and the Email 2 network [45] with $n = 3188$. As the greedy algorithm is prohibitively slow for large networks, we drop it and instead compare the proposed algorithm with a randomly sampled seed set. Additionally, since the BOPIM algorithm performed similarly across shrinkage priors in the experiments in the main manuscript, we only consider the Horseshoe prior here.

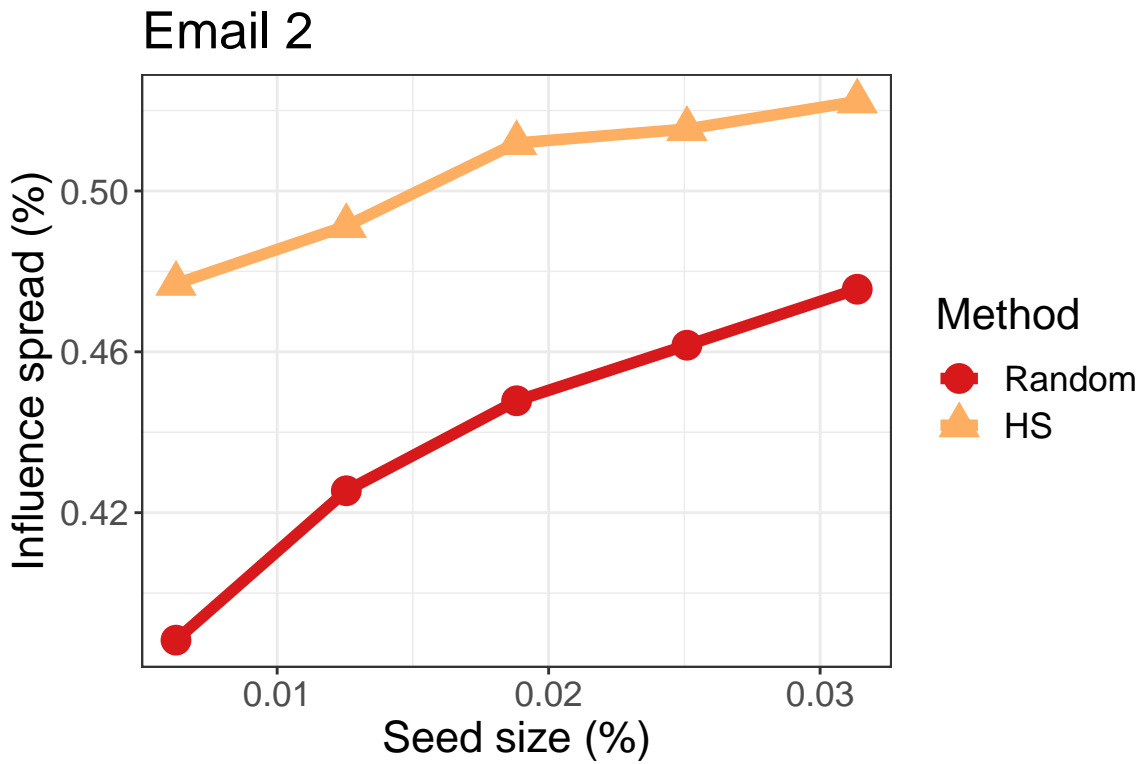
For both networks, we fix $\lambda = 0.05$ and $T = 10$, and vary $k = 20, 40, \dots, 100$. All other settings and hyperparameters are the same as in the main manuscript. The results for influence spreads are in Figures 6a and 6b and for computation times in Figures 7a and 7b. It's clear that the proposed method yields superior influence spread compared to random seeding, while the computations are performed in a reasonable amount of time.

5.3 Uncertainty quantification

In Section 3.4 of the main manuscript, we look at uncertainty quantification (UQ) for the DL prior on the Reality network. Here, we present the same results for the Horseshoe and R2D2 prior in Figures 8 and 9, respectively. For the Horseshoe prior, we notice that node 1 has a very large posterior distribution, but every other coefficients is centered close to 0. Indeed, from Figure 8(b), we can see that many nodes have similar proportions. Additionally, the posterior distributions all appear to have a fairly large variance. Conversely, for the R2D2 prior, the posterior distributions have a very small variance and there are four nodes which clearly should be included in the seed set. The fifth most influential node appears to be far less influential and has several comparable candidates. Interestingly, even though the IM results are very similar across the three shrinkage priors, their posterior distributions are vastly different as evidenced by these figures.

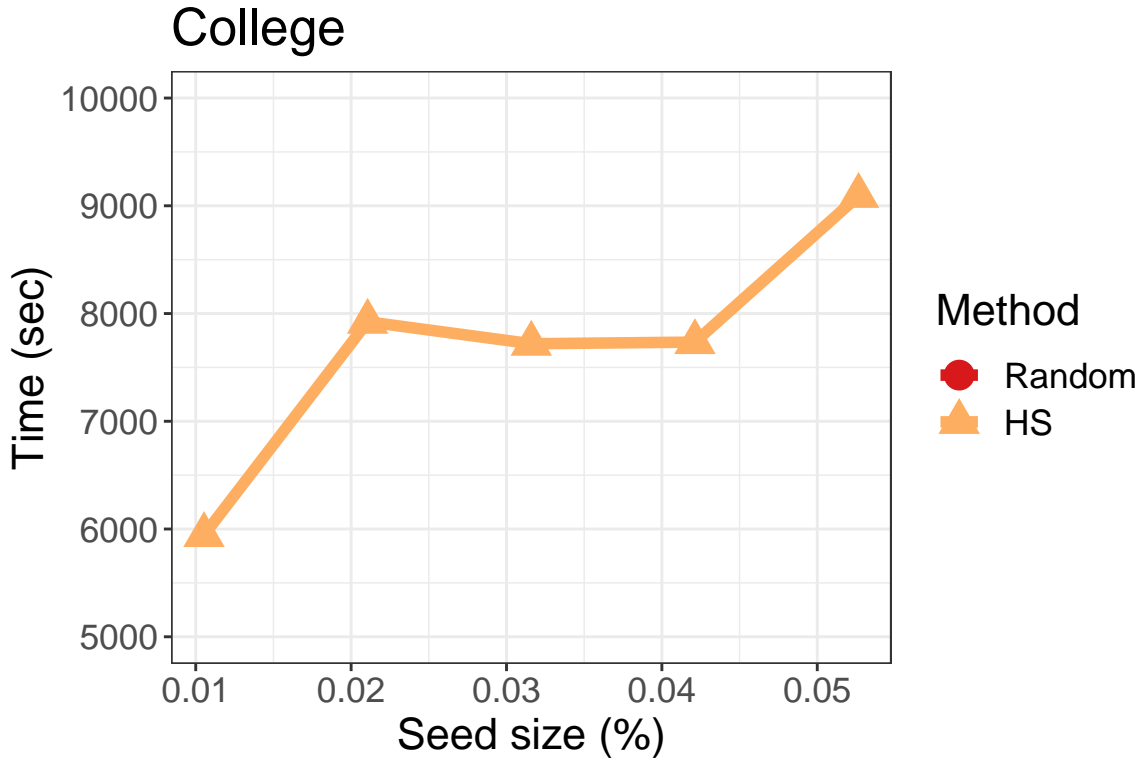


(a) College network

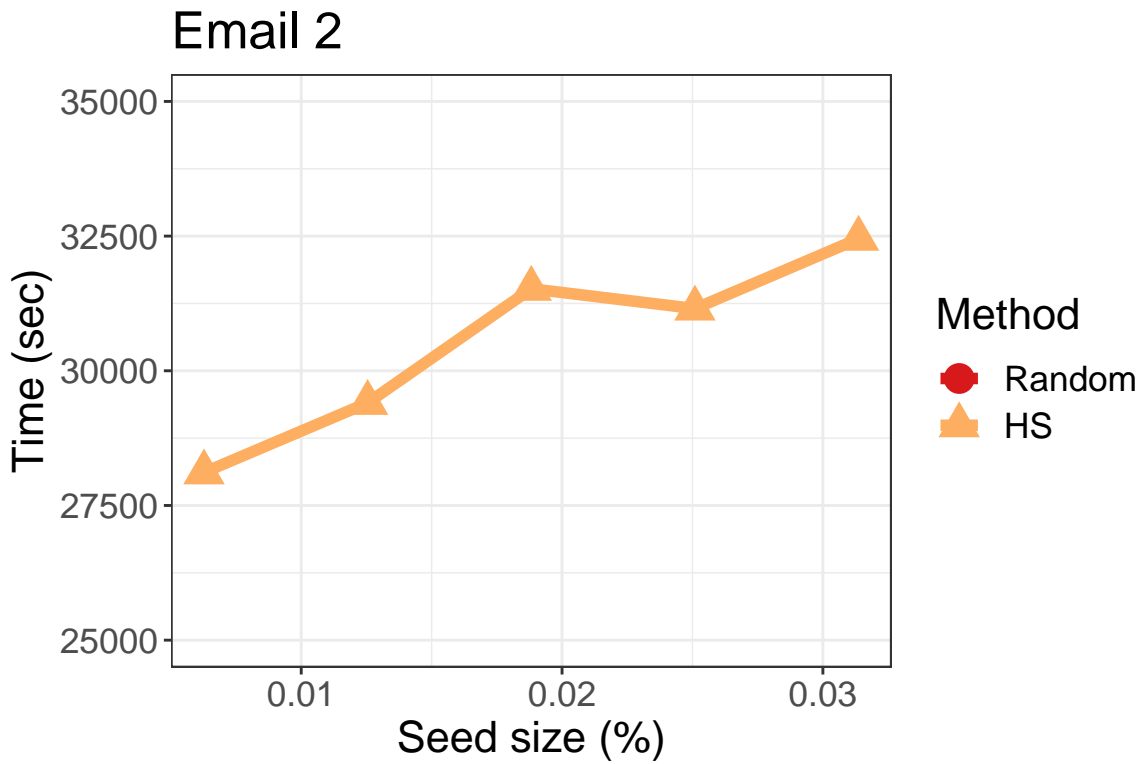


(b) Email 2 network

Figure 6: Influence maximization results for the College and Email 2 networks.

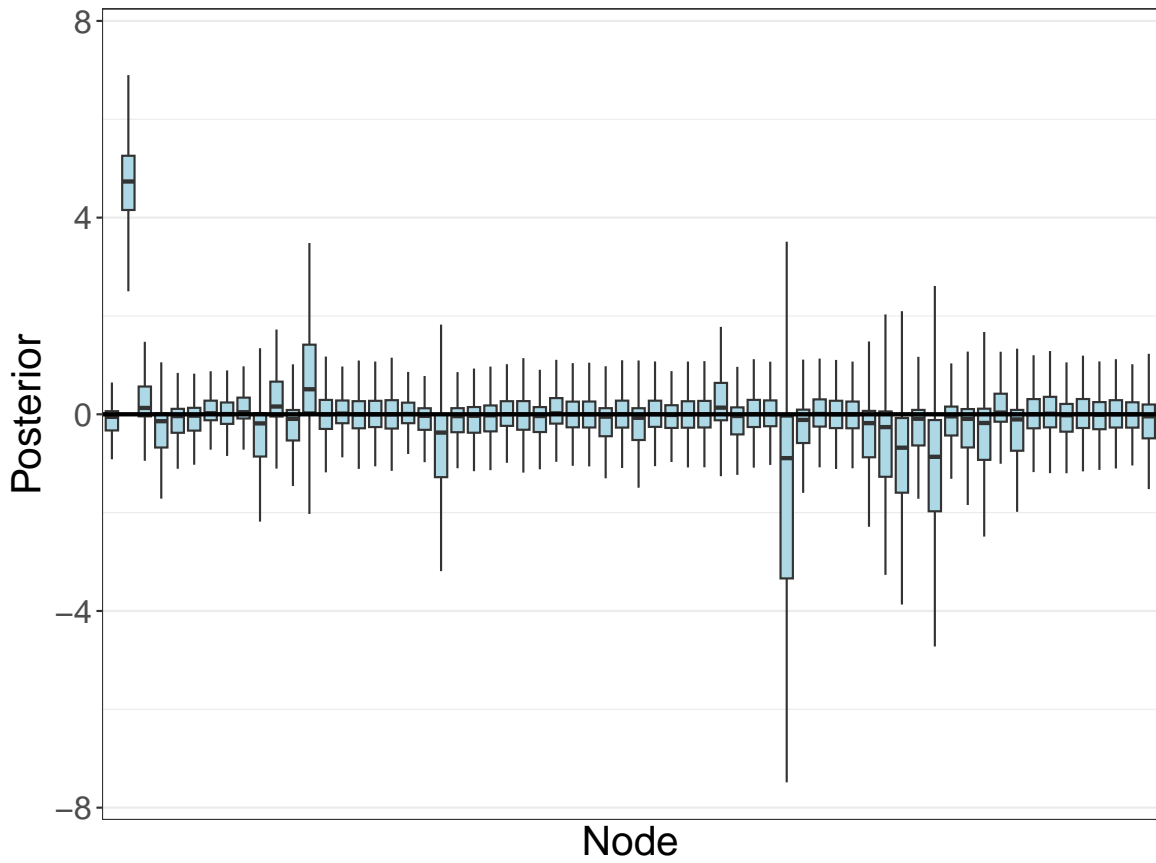


(a) College network

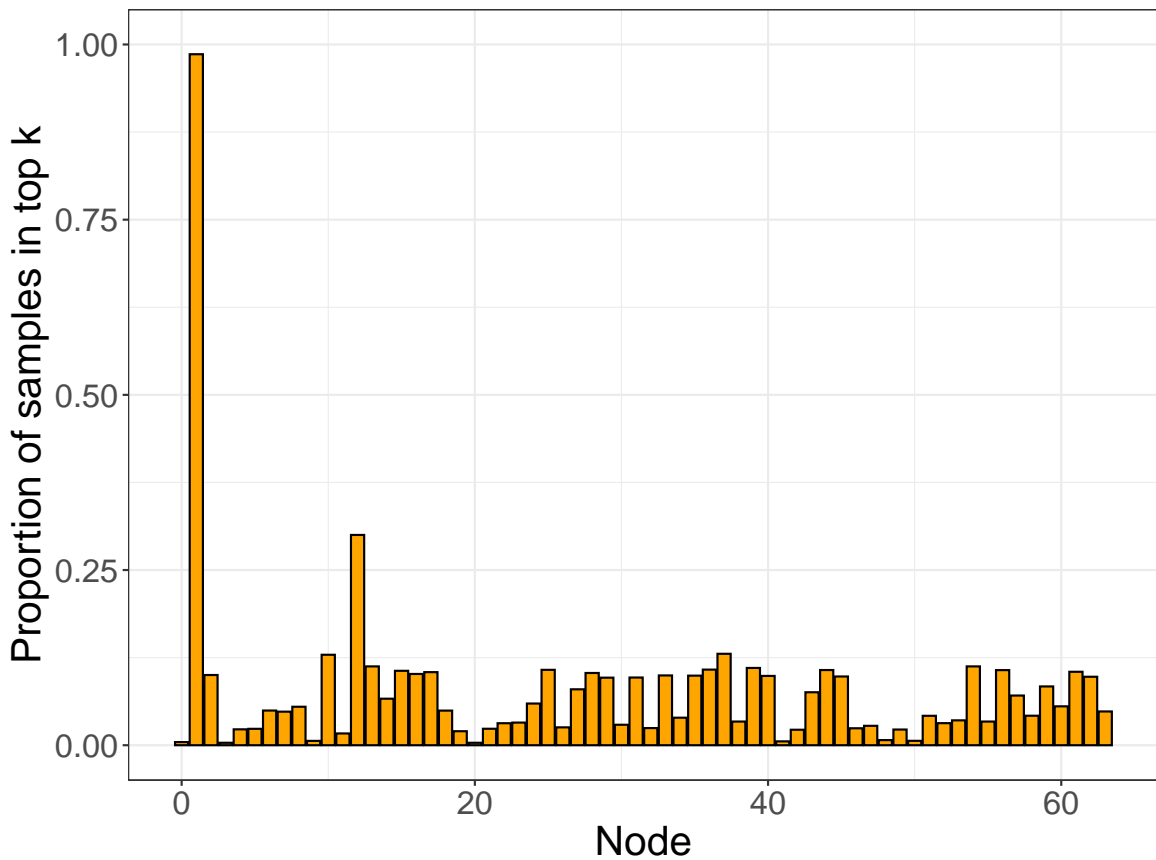


(b) Email 2 network

Figure 7: Computational results for the College and Email 2 networks.

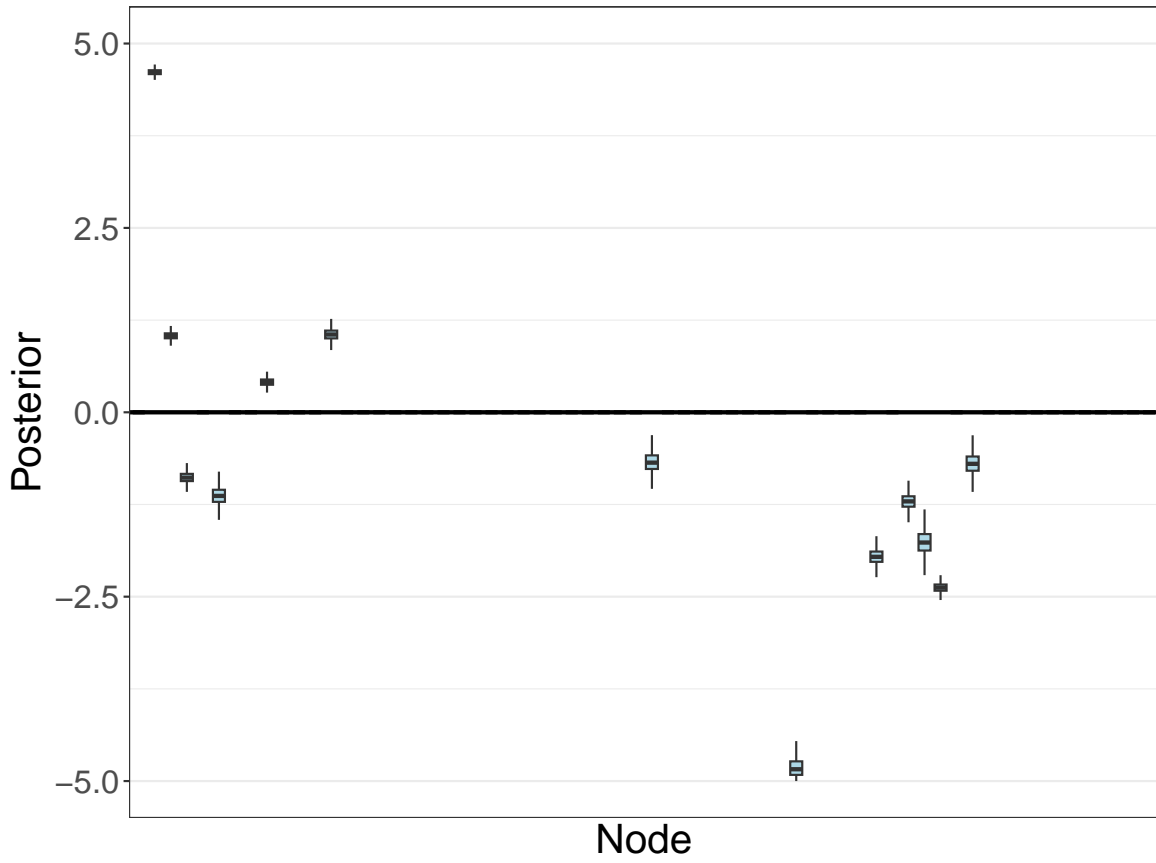


(a) Posterior distribution box plots.

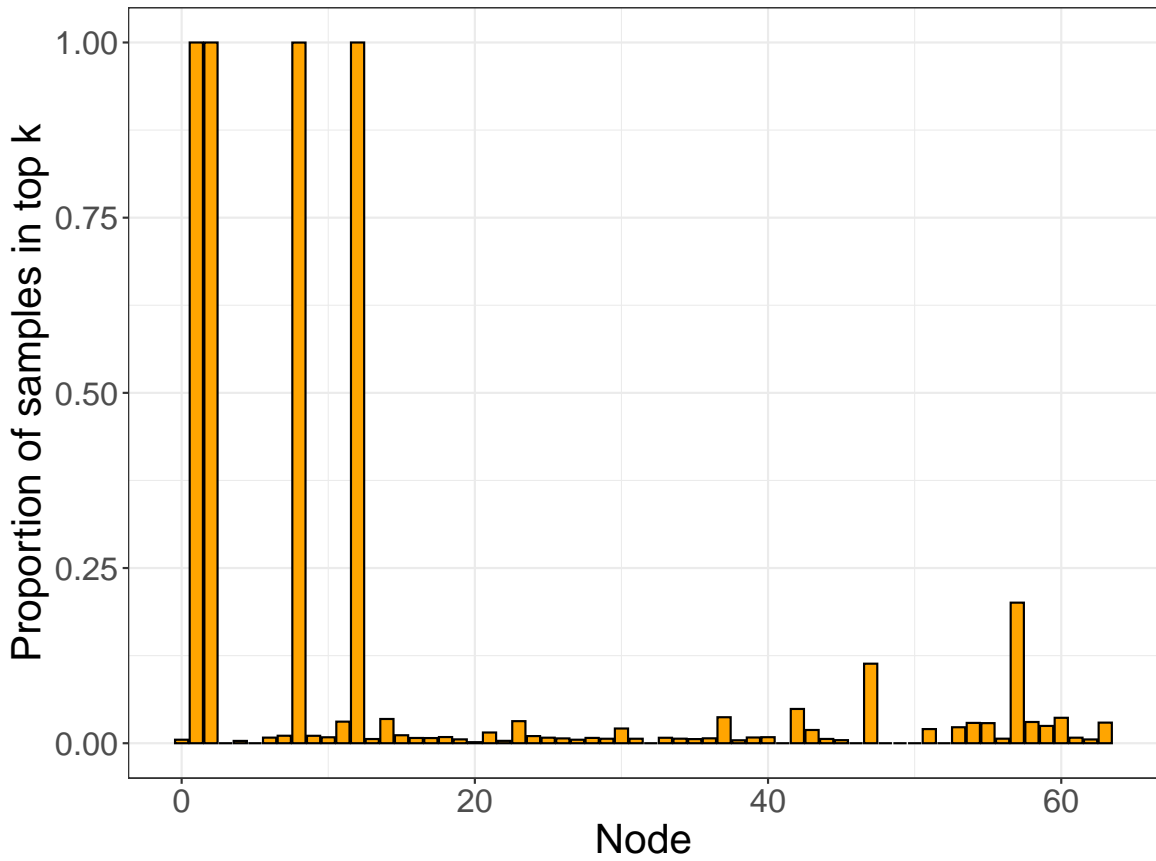


(b) Proportion of MCMC samples in top k .

Figure 8: Posterior distribution summaries for Horseshoe prior and Reality network.



(a) Posterior distribution box plots.



(b) Proportion of MCMC samples in top k .

Figure 9: Posterior distribution summaries for R2D2 prior and Reality network.